up to 104%. Hence, the reflecting–equalizing electromagnetic field system available in the "Slavyanka" furnace only partly solves the problem of the elimination of the nonuniformity of the field distribution of the resonator, which is one of the basic products in the processes of thermal treatment. Evidently, the methods of "equalization" of a multimode uhf field of standing waves should be combined, providing simultaneous displacement of the product and the field with respect to each other.

NOTATION

dW, energy released in the calorimater; $d\bar{t}$, average temperature variation; c_w and c_c, specific heats of the water and of the calorimeter; m_w and m_c, masses of the water and of the calorimeter; p_t, total specific power of the multimode electromagnetic field (the energy generated in an element of volume ΔV during time $d\tau$); f_g, frequency of the generator; E_{ef}, effective vector of the intensity of the electric component of the field in the volume element ΔV; $\varepsilon''_{t.w}$, total loss factor of the water; ρ_w, density of water; B, a quantity that depends on the frequency of the generator; v_t, rate of heating of the liquid; ε_{E^2} and ε_{pt}, relative nonuniformities in the distribution of the square of the intensity and the total specific power in the resonator.

LITERATURE CITED

1. A. S. Zusmanovskii and Yu. V. Leibin, "Design and construction of rectangular resonator chambers for devices for uhf heating of dielectrics," Elektron. Tekh., Ser. 1, Elektron. SVCh, No. 8, 72-81 (1968).
2. Yu. K. Gubiev, A. G. Gasparyants, and V. V. Krasnikov, "Scattering of a multimode uhf field in a moist dielectric," Inzh.-Fiz. Zh., 36, No. 6, 1116 (1979).
3. Yu. K. Gubiev, "Investigation of the process of heating of liquid food products in a multimode uhf field," Author's Abstract of Candidate's Dissertation, Technical Sciences, Moscow (1975), pp. 7-9.

CALCULATION OF THE TEMPERATURE PATTERNS IN CONTINUOUS CASTING OF CERAMIC COMPONENTS FROM THERMOPLASTIC SLIP

E. V. Nomofilov, Yu. V. Dvinskikh, R. Ya. Popil'skii, V. V. Kulagin, and S. I. Morozova

UDC 666.3.022:536.24

A method is given for calculating the parameters and temperature patterns in continuous hot casting of ceramic components. The calculations are in satisfactory agreement with experiment.

Continuous casting of ceramic components from thermoplastic slip is widely used [1, 2]. This method is mainly used when one requires long tubular precision components of multilayer type with single or multiple channels. The thermophysical processes occurring in this form of casting are similar to those in the continuous forming of metals and alloys [3], but they are more rapid and occur on the shorter parts of the system, while the thicknesses and the temperature gradients are much smaller than those in forming metals. This causes certain difficulties in examining the solidification of the slip, which is necessary in choosing or calculating the parameters.

The basic parameters determining the throughput are the casting rate and the cooling rate. It is therefore necessary to know the temperature distributions.

Existing analytic methods are complicated or of low accuracy [3-5]. Here we give a method of calculating the temperature distributions in solidifying the solidified slip.

Power Physics Institute, Obninsk. Translated from Inzhenerno-Fizicheskii Zhurnal, Vol. 40, No. 6, pp. 1075-1082, June, 1981. Original article submitted December 24, 1979.

0022-0841/81/4006-0654$07.50

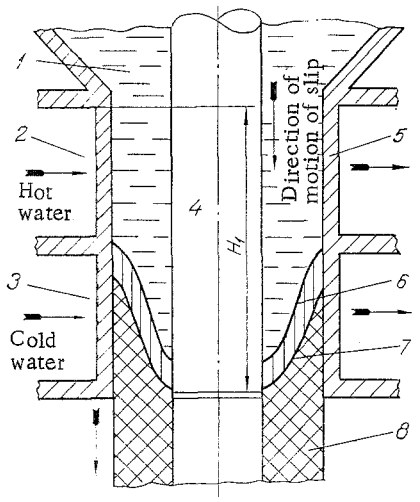

Fig. 1

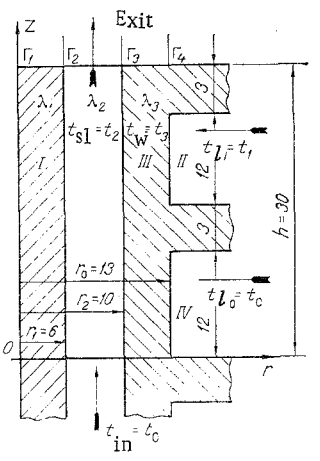

Fig. 2

Fig. 1. Moulding heat-exchange die for casting a circular tube: 1) liquid slip; 2) hot zone; 3) cold zone; 4) internal crystallizer; 5) external crystallizer; 6) 54°C isotherm; 7) 48°C isotherm; 8) solid slip (component).

Fig. 2. Working cylindrical system: I) internal crystallizer (rod); II) cold zone; III) external crystallizer; IV) hot zone.

This method allows one to calculate the isotherms, the parameters, and the basic geometrical dimensions of the heat-transfer dies.

There are three zones in continuous casting from thermoplastic slip, as in the casting of metals and alloys [3, 4]: liquid, liquid–solid, and solid, which are separated by isothermal solidus and liquidus surfaces (see the scheme for a circular tube in Fig. 1). Also, the law followed by the solidification front is the same whether or not there is a crystallization temperature range. Therefore, the solidification front is to be determined from the melting point, while the width of the solidification zone is taken as zero. The following assumptions were also made:

1) the process was considered stationary. In fact, the temperature fluctuations in the wall and vessel are not more than 0.5-1°C [3, 5];

2) the heat released in crystallization is neglected, since this is small by comparison with the total amount of heat to be removed during cooling. The content of unsolvated bonding agent in the system is small (about 5%), while the solvated part of the bonding agent hardly alters in state of aggregation [6];

3) the heat transfer between the surrounding medium and the die is neglected, because the water temperature is almost the same as that of the surroundings in the cold zone of the die;

4) heat transfer between the hot and cold zones of the die is neglected;

5) the heat-transfer coefficient from the water to the wall of the crystallizer is constant at all points in the height of the cold zone;

6) the heat transfer between the component and the air on exit from the die is neglected as being negligibly small; and

7) as the process is stationary, the die is in adiabatic conditions.

We calculated a cylindrical system with an internal steel solid cylinder of radius r_1, an annular gap for the slip $r_2 - r_1$, an outer steel cylindrical wall $r_0 - r_2$, and a total height for the crystallizer H (Fig. 2). The temperature t_0 of the hot water and slip was taken as 80°C; the end of crystallization or solidification was determined by the method of [7] as $t_{sol} = 48$°C; the cold water in the experimental system was in the range $0 \leqslant t_{l_1} \leqslant 35$°C. The calculation gave the position of the t_{sol} isotherm, for which purpose we deter-

mined the temperature distribution over the radius and along the length. We solved the equation of thermal conduction for the cylindrical systems, which took the following form:

$$a\left[\frac{\partial}{\partial r}\left(r\frac{\partial t}{\partial r}\right)+\frac{\partial^2 t}{\partial Z^2}\right]=W\frac{\partial t}{\partial Z}. \tag{1}$$

The condition of equal temperatures was assumed for the slip–wall boundary. The thermal conductivities λ were independent of temperature (for steel, the variation in λ in this temperature range is in fact small, while for slip it is dependent in the main on the thermal conductivity of the bonding agent, and the difference in λ in the range 20-80°C is indicated by experiment as only 3 W/m·deg); the speed of the liquid slip was considered the same at all radii because the gaps in the dies are very small; a condition of the third kind was specified at r_0. The boundary conditions took the following form (for symbols see Fig. 2):

$$1)\ \left.\frac{\partial t}{\partial r}\right|_{r_1}=0,\quad 2)\ t_{\text{in}}=t_0,\quad 3)\ \left.\frac{\partial t}{\partial Z}\right|_{\text{exit}}=0,$$

$$4)\ \lambda_3\left.\frac{\partial t}{\partial r}\right|_{r_1}=\alpha_s(t_w-t_{l_s}),\ \text{where}\ n=0;\ 1\ \text{(condition of the 3rd kind)},$$

$$\left.\begin{aligned}5)\ \lambda_1\left.\frac{\partial t_1}{\partial r}\right|_{r_2}&=\lambda_2\frac{\partial t_2}{\partial r},\quad t_1=t_2,\\ \lambda_2\left.\frac{\partial t_2}{\partial r}\right|_{r_3}&=\lambda_3\frac{\partial t_3}{\partial r},\quad t_2=t_3\end{aligned}\right\}\ \text{— link equations.}$$

The M-220 has only limited memory, so we considered a two-dimensional formulation, which is quite acceptable for restricted wall thicknesses (as occurs in casting ceramic components), while the system had a symmetry axis, so the calculation was performed only for half of it (Fig. 2). To eliminate the dependence of the solution on the geometrical dimensions, (1) and the boundary conditions were converted to dimensionless form. The following dimensionless variables were introduced:

$$R=\frac{r}{r_0},\quad \tilde{Z}=\frac{Z}{H},\quad \tilde{\alpha}=\frac{\alpha_s}{\alpha_0};\quad \text{Pe}=\frac{Wr_0}{a};\quad t=\frac{t}{t_0};$$

$$\text{Bi}=\frac{\alpha_s r_0}{\lambda_3};\quad \tilde{\lambda}_m=\frac{\lambda_i}{\lambda_2},$$

where i = 1, 2, 3 are the numbers of the zones. Then (1) and the boundary conditions become

$$\frac{\partial^2 t}{\partial R^2}+\frac{1}{R}\frac{\partial t}{\partial R}+\frac{\partial^2 t}{\partial \tilde{Z}^2}=\text{Pe}\frac{\partial t}{\partial \tilde{Z}}, \tag{2}$$

$$1)\ \left.\frac{\partial t}{\partial R}\right|_{r_0}=0,\quad 2)\ t_{\text{in}}=1,\quad 3)\ \left.\frac{\partial t}{\partial \tilde{Z}}\right|_{\text{exit}}=0,$$

$$4)\ \tilde{\lambda}_m\left.\frac{\partial t}{\partial R}\right|_{r_0}=\text{Bi}(t_w-t_{l_s}),$$

$$\left.\begin{aligned}5)\ \tilde{\lambda}_m\left.\frac{\partial t}{\partial R}\right|_{r_2}&=\frac{\partial t}{\partial R},\quad t_1=t_2,\\ \left.\frac{\partial t}{\partial R}\right|_{r_3}&=\tilde{\lambda}_m\frac{\partial t}{\partial R},\quad t_2=t_3.\end{aligned}\right\}$$

A finite-difference method [8, 9] was used to solve the system. The region of variation was split up as a square net with step h; $R_i = ih$; $Z_i = kh$. The equation was approximated with accuracy $O(h^2)$, while the boundary conditions were approximated with accuracy $O(h)$, and then the iteration equation takes the form

$$-f_{i,k}t_{i,k}+b_{i,k}t_{i,k-1}+a_{i,k}t_{i-1,k}+\alpha_{i,k}t_{i,k+1}+C_{i,k}t_{i+1,k}=0, \tag{3}$$

where

$$f_{i,k}=\frac{4}{h^2};\ b_{i,k}=\left(\frac{1}{h}+\frac{\mathrm{Pe}}{2}\right);\ a_{i,k}=\left(\frac{1}{h}-\frac{1}{2R}\right);\ C_{i,k}=\left(\frac{1}{h}+\frac{1}{2R}\right);\ d_{i,k}=\left(\frac{1}{h}-\frac{\mathrm{Pe}}{2}\right).$$

Equation (3) was used with the boundary conditions also written in terms of finite differences as the initial system of algebraic equations, which was solved numerically by computer.

The temperature distribution in the given region was derived. From the temperature distribution we determined the isotherms and determined the maximum height at which the slip was completely solidified, i.e., we determined the depth H_1 of the solidified slip (Fig. 1), which was proportional to the linear velocity. Consequently, the maximum permissible velocity is dependent on the thickness of the component and the depth of the pit and corresponds to the height of the crystallizer in the cold zone [10].

Therefore, it is important to determine not only the positions of the isotherms but also the relationship between the basic parameters: casting rate, pit depth, wall thickness, and heat-transfer conditions in the die. The solution then enables one to determine the parameters of the process and the basic geometrical dimensions of the die.

We calculated H_1 with the following values: t_{l_1} = 0; 0.1; 0.225; 0.3125; 0.375; 0.414; 0.475; Pe = 0.05-0.8; Bi 1-40, and from the values of H_1 we derived the general formula

$$H_1=Ae^{Bt_{l_1}}+G. \tag{4}$$

Parameters A, B, and G were found by least-squares fitting, and these are functions of Pe and Bi, so the next stage was to find simple formulas for these parameters with adequate accuracy:

$$B=(1.17\arcsin\mathrm{Pe}+3.24)\,I_0\left(\frac{1}{\mathrm{Bi}}\right)+(0.046-1.065\arcsin\mathrm{Pe}). \tag{5}$$

$$A=-(0.0392^{-\mathrm{Pe}}\cos\mathrm{Pe}-0.099)\ln\mathrm{Bi}+(2.074+0.2585\,e^{-\mathrm{Pe}}), \tag{6}$$

$$G=A'\ln\mathrm{Bi}+C'I_0\left(\frac{1}{\mathrm{Bi}}\right)+\mathrm{B}', \tag{7}$$

$$A'=-1.595\,I_0(\mathrm{Pe})+0.562\,I_1(\mathrm{Pe})+1.838, \tag{8}$$

$$C'=-3.812\,I_0(\mathrm{Pe})\cos\mathrm{Pe}-0.997\,I_1(\mathrm{Pe})\,e^{-\mathrm{Pe}}+6.366, \tag{9}$$

$$B'=11\exp^{(0.55-\mathrm{Pe})[-0.0226+0.1944\ (0.55-\mathrm{Pe})]}, \tag{10}$$

where I_0 and I_1 are Bessel functions.

A check showed that the maximum deviation of (4) from the theoretical curves was 6% under the following conditions: $0\leqslant t_{l_1}\leqslant 0.4375$, $10^{-5}\leqslant\mathrm{Pe}<1$, $1\leqslant\mathrm{Bi}\leqslant 40$; for parger Pe we derived the empirical relationship

$$H_1=a'\,\mathrm{Pe}+a'', \tag{11}$$

where

$$a'=a_0'I_1\left(\frac{1}{\mathrm{Bi}}\right)+b_0'; \tag{12}$$

$$a''=a_0''I_1\left(\frac{1}{\mathrm{Bi}}\right)+b_0''; \tag{13}$$

$$a_0'=15.05\,(t_{l_1})^{2.7}+1.03; \tag{14}$$

$$b_0'=1.295\,(t_{l_1})^{2.3}+0.42736; \tag{15}$$

$$a_0''=22.5\,(t_{l_1})^{1.55}-0.6084; \tag{16}$$

$$b_0''=16.55\,(t_{l_1})^{1.55}+16.25. \tag{17}$$

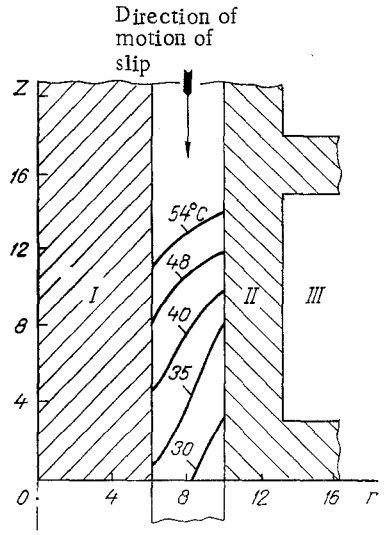

Fig. 3

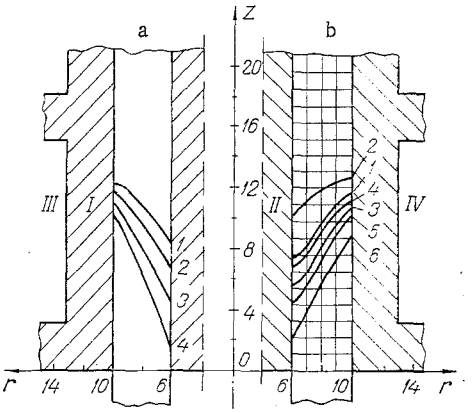

Fig. 4

Fig. 3. Temperature distribution in the cold zone of experimental die during casting with $t\zeta_1 = 0.25$; Pe = 1.63; Bi = 1.4: I) internal crystallizer; II) outer; III) cold zone; Z distance from lower end of die in mm; and r distance from axis of die in mm.

Fig. 4. Position of the isotherm for end of solidification (t_{sol} = 48°C = 0.6 t_0) during casting: a) experimental data for Bi = 0.98; $t\zeta_1 = 0.25$ [1) for Pe = 1.63; 2) 3.26; 3) 4.89; 4) 6.52]; b) calculated data for Bi = 4.55; $t\zeta_1 = 0.25$ (1 for Pe = 1.63 from (4); 2 for the value 3.26 from (11); 3 for 3.26 from (4); 4 for 4.89 from (11); 5 for 6.52 from (11); 6 for Pe = 8.15 from (11)); I) outside crystallizer; II) internal; III and IV) cold zones.

A check showed that the maximum deviation of (11) from the theoretical curves was not more than 1% for $1 \leqslant Pe \leqslant 9$; $0.05 \leqslant t\zeta_1 \leqslant 0.3125$; $2 \leqslant Bi \leqslant 40$, the following corrections were made to (11):

$$a_0' = 18{,}8\,(t_{l_1})^{2,9} + 1{,}0365, \tag{18}$$

$$a_0'' + 25{,}96\,(t_{l_1})^{1,7} - 0.4898. \tag{19}$$

The corrections are applicable provided that the $d_{i,k}$ in (3) remains positive: $d_{i,k} = \left(\frac{1}{h} - \frac{Pe}{2}\right) > 0$.

Comparison of the calculated curves with experiment showed that the results from (4) gave H_1 too low by 9.5%, while (11) gave values too high by 14%, which is quite satisfactory for practical purposes.

The experimental data were obtained on a die with geometrical parameters corresponding to the calculation system (Figs. 1 and 2). To record the temperatures in the crystallization zone, the inner and outer surfaces of the crystallizer in contact with the slip were fitted to a depth of 0.3 mm with Chromel–Copel thermocouples. The thermocouples were arranged with a step of 3 mm in height and at intervals of 90° around the section. Extreme values of the isotherms were constructed from 3-7 points, which were determined in accordance with the data of [11] on the assumption that the temperature varies linearly in these short gaps (3-4 mm). Figures 3 and 4 show some results and experimental data obtained with the die.

The following must be borne in mind for practical purposes. When other dies are constructed, the new geometrical parameters $r_{1,x}$, $\lambda_{1,x}$, $r_{0,x}$, $r_{2,x}$, $\lambda_{3,x}$ must relate to parameters used in the calculations as $\frac{r_1}{\lambda_1} = \frac{r_{1,x}}{\lambda_{1,x}}$, i.e., we must have

$$\frac{r_{1,x}\lambda_1}{\lambda_{1,x}r_1} \geqslant 1 \text{ and } \frac{(r_{0,x}-r_{2,x})\lambda_3}{\lambda_{3,x}(r_0-r_2)} \geqslant 1. \tag{20}$$

The outside diameter of the die not used in the calculation is considered as an adiabatic shell, and this can be taken on the basis of the specification or by calculation for Bi.

When the parameters of the new system have been fitted to (20), one determines Pe and Bi:

$$\mathrm{Pe} = \frac{Wr}{a}, \tag{21}$$

$$\mathrm{Bi} = \frac{\alpha_n r}{\lambda}, \tag{22}$$

where W is specified or is defined from the other parameters in (4) and (11); a is found by experiment and it can also be calculated with satisfactory accuracy via λ from Russel's formula [12]; α_n is calculated by Mikheev's method for a transverse flow around a single cylinder [12, 13] via the Nusselt number:

$$\alpha_n = \mathrm{Nu}_f \frac{\lambda_f}{2r}. \tag{23}$$

The Nusselt number Nu_f is determined from the Reynolds and Prandtl numbers via the following formulas: for $\mathrm{Re}_f = 1\cdot10^1\text{-}1\cdot10^3$

$$\mathrm{Nu}_f = 0.5\,\mathrm{Re}_f^{0.5}\,\mathrm{Pr}_f^{0.38}\left(\frac{\mathrm{Pr}_f}{\mathrm{Pr}_w}\right)^{0.25}, \tag{24}$$

and for $\mathrm{Re}_f = 1\cdot10^3\text{-}2\cdot10^5$

$$\mathrm{Nu}_f = 0.25\,\mathrm{Re}_f^{0.6}\,\mathrm{Pr}_f^{0.38}\left(\frac{\mathrm{Pr}_f}{\mathrm{Pr}_w}\right)^{0.25}, \tag{25}$$

where f denotes the liquid at the inlet to the system and w the same at the outlet.

It has been pointed out that the water temperatures at the inlet and outlet differ only slightly, so the $(\mathrm{Pr_f}/\mathrm{Pr_w})^{0.25}$ factor is close to one and is neglected in the calculation.

$\mathrm{Pr_f}$ has been tabulated:

$$\mathrm{Re}_f = \frac{Vd}{\nu_f}. \tag{26}$$

Therefore, (4) and (11) supplement one another and relate the geometrical parameters of the system (H, r_0, r_1, r_2) to the basic parameters of the casting process (Bi, Pe, $t\zeta_1$, H_1), any of which can be specified or defined by a simple calculation on the basis of the thermophysical parameters of the thermoplastic slip.

NOTATION

r, variable radius; r_0, r_1, r_2, radius of envelope; t, dimensionless temperature; a, thermal diffusivity; W, velocity in die; V, water velocity in the envelope; Z, variable longitudinal coordinate; λ, thermal conductivity; α, liquid-to-wall heat-transfer coefficient; $\tilde{\alpha}$, dimensionless liquid-to-wall heat-transfer coefficient; R, dimensionless radius; $\tilde{Z}$, dimensionless longitudinal coordinate; H, envelope height; H_1, depth of hole in solidified slip; I_0, I_1, zero- and first-order Bessel functions; ν, kinematic viscosity; Pe, Péclet number; Bi, Biot number; Nu, Nusselt number; Re, Reynolds number; Pr, Prandtl number. Indices: sol, crystallization; l, liquid; Γ_1, Γ_2, Γ_3, Γ_4, boundaries of calculated envelopes; in, inlet; w, wall; f, liquid at inlet; w, liquid at exit; s, slip; i, number of step along the abscissa; k, number of step along the ordinate.

LITERATURE CITED

1. I. F. Usatikov, "A pure-oxide microsleeve," Nauchnye Trudy UNIIO [in Russian], Issue 13, Metallurgiya, Moscow (1970), pp. 169-173.
2. D. N. Poluboyarinov and R. Ya. Popil'skii (eds.), Ceramics from Refractory Oxides [in Russian], Metallurgiya, Moscow (1977).

3. R. M. Gabidullin et al., "Computer calculations of the temperature distributions in continuous casting," Tekhnol. Legkikh Splavov, No. 4, 50-54 (1973).
4. A. I. Veinik, Theory of Special Forms of Casting [in Russian], Mashgiz, Moscow (1958).
5. B. Chalmers, Principles of Solidification [Russian translation], Metallurgiya, Moscow (1968).
6. Yu. V. Dvinskikh, L. I. Kostin, and V. V. Kulagin, Inventor's Certificate No. 390417, "Method of determining the adsorption capacity of materials," Deposited 25.02.71 as No. 1626645, Byull. Izobret., No. 30, class G01n13/00, G01n31/06 (1973).
7. P. O. Gribovskii, Hot Casting of Ceramic Components [in Russian], Énergoizdat, Moscow—Leningrad (1961).
8. A. A. Samarskii, An Introduction to the Theory of Difference Schemes [in Russian], Nauka, Moscow (1971).
9. B. P. Demidovich, I. A. Maron, and É. Z. Shuvalov, Numerical Analysis Methods [in Russian], Nauka, Moscow (1967).
10. M. S. Boichenko, V. S. Rutes, and V. V. Ful'makht, Continuous Casting of Steel [in Russian], Metallurgizdat, Moscow (1961).
11. P. P. Budnikov and N. V. Shishkov, "Theory of the crystallization of thermoplastic slip during casting," Prikl. Khim., 35, No. 2, 272-283 (1963).
12. A. F. Chudnovskii, Thermophysical Characteristics of Disperse Materials [in Russian], Fizmatgiz, Moscow (1962).
13. M. A. Mikheev and I. M. Mikheeva, A Short Textbook on Heat Transfer [in Russian], Gosenergoizdat, Moscow—Leningrad (1961).

HEAT-FLOW DISTRIBUTION AND COMBINED HEAT—MASS TRANSFER PROCESSES AT THE CONTACT INTERFACE OF A FRICTION PAIR

V. A. Balakin

UDC 539.621:536.12

The processes of heat release, heat-flow distribution, and combined heat—mass transfer in sliding contact are analyzed on the basis of measurements of the heat flux directed into one member of a friction pair.

The solution of a number of engineering problems bearing on the need to increase the operational reliability and wear resistance of heavily loaded and high-speed friction components in machines and instruments requires investigation of the laws governing heat exchange (heat-flow distribution) and combined heat—mass transfer at a sliding-contact interfact between bodies.

The primary objective here is to determine the working thermal regime of a friction pair (average temperature of the friction surface and the temperature fields relative to frictional contact) as well as to ascertain the causes of wear and the times at which it occurs [1, 2]. Friction thermal problems are solved by the methods of heat-conduction theory under Neumann boundary conditions. As a rule, the specific rate of heat release per unit nominal contact area of the bodies at any instant is known (from measurements of the instantaneous values of F and v) and is given by the equation

$$q = fp_a v.$$

However, to properly account for the heat distribution in frictional contact and, hence, to decide the correct boundary conditions for the solution of friction thermal problems presents considerable difficulty, particularly under the conditions of unsteady heat release, variation of the spacing of the mating friction pair, and combined heat—mass transfer (transfer of heated surface layers from one body to the other). The values of the heat-flow distribution coefficient $\alpha = q_{a_1}/q$ are customarily determined analytically [3]. Expressions for the calculation of α, e.g., in the case of contact between flat bodies are

Gomel State University. Translated from Inzhenerno-Fizicheskii Zhurnal, Vol. 40, No. 6, 1083-1089, June, 1981. Original article submitted December 17, 1979.

 0022-0841/81/4006-0660$07.50